

Nima Zoghipour* 

Ferhat Çelik 

Torun Bakır Alaşımları
Metal San. Ve Tic. A.Ş.
Kocaeli/Türkiye

Yusuf Kaynak 

Marmara Üniversitesi
Makine Mühendisliği Bölümü
İstanbul/Türkiye

Makale Bilgisi:

Araştırma Makalesi

Gönderilme: 04-02-2020

Kabul: 26-04-2021

*Sorumlu Yazar: Nima Zoghipour
Email: nima.zoghipour@gmail.com

Optimization of Process Parameters in Drilling Process of Forged Ecofriendly Low-Lead Brass Alloy

This research presents an experimental investigation of the drilling operation on surface integrity characteristics of forged eco-friendly low-lead brass alloy using flat bottom drill cutting tool and application of techniques for order preference by similarity to ideal solution (TOPSIS) and Grey relational analysis methods in parametric optimization for solving multiple criteria (objective) process. Experimental data on dimensional accuracy, machining time, cutting forces, and the surface quality of the holes are analyzed to evaluate surface integrity of machined specimens. Analysis of variance (ANOVA) was performed to dispose the significance of the parameters at a %95 confidence interval. Both optimization tools resulted in the same cutting parameters. The analysis of the obtained chip forms verifies the optimization results.

Keywords: TOPSIS, Grey relation analysis, optimization.

INTRODUCTION

Brass is an alloy of copper and zinc, in extents which can be differed to accomplish shifting mechanical, metallurgical and electrical properties [1]. This alloy is perceived for its high strength, high ductility, wear resistance, high electrical and thermal conductivity, recyclability, antibacterial and hygienic, corrosion resistance, and good machinability. Most of all the conveyed brass metal is ought to be machined into its net shape and size. Such tasks generally consolidate cutting operations for different sorts including drilling, turning, milling, grinding, etc. [2]. Lead is regularly added around %2 into brass composition in order to increase the machinability of brass. Lead has a low solubility, and it can migrate towards the grain boundaries in the form of globules as it cools from casting and segregate in the entire microstructure and grain boundaries. Moreover, low melting temperature, $T_m=327.5^\circ\text{C}$ leads to behave as a lubricant during machining [2]. In addition, cutting operations can smear the lead globules over the surface. These effects can lead to significant lead leaching from brasses of comparatively low lead content [3]. From an absolutely manufacturing monetary outlook, replacement of lead-containing

metal with a low-lead or lead-free elective does not have all the earmarks of being a financially feasible alternative, yet it is in fact conceivable, fulfilling the prerequisites of the authorized enactment. However, as an increasing amount of low-lead and lead-free brasses are becoming commercially available and future legislative actions could be expected, even further limiting the use of lead as an alloying element, there is a renewed interest in evaluating the machinability of these new low-lead and lead-free materials [4].

Rahman et al. [5] carried out a study on optimum drilling parameter for HSS drilling tool in micro-drilling processes considering the effect of drilling parameter such as spindle speed, feed rate and drilling tool size on material removal rate (MRR), surface roughness, dimensional accuracy and burr in order to find the best drilling parameter for brass as a workpiece material. Timata et al. [6] carried out an experimental study in drilling forging brass using a special tungsten carbide drilling tool. They studied the exit burr height and workpiece diameter at different spindle speeds and feed rates and used ANOVA in their study. Their ANOVA results demonstrated that

spindle speed and feed rate on exit burr height and workpiece diameter were statistically at significant of level. Kato et al. [7] investigated the effects of web thinning, the helix angle, and the nick geometry on chip evacuation by drilling small holes in lead-free brass with a micro drill. Their results showed that drills with a helix angle of 15° have the longest tool life. Youssef et al. [8] conducted a design of experiment approach to examine the effect of feed rate, rotational speed, drill diameter, and thickness of work material as process variables on the burr formation. The effect of the burr formation on the hardness of the exit surface of the drilled workpiece was investigated by them. Hua et al. [9] studied the impacts of cutting-edge geometry, and workpiece hardness, cutting conditions such as feed rate and cutting speed. They indicated that sharpened edge in addition to chamfer cutting edge and higher feed rate help to increment both compressive residual stress, hardness and penetration depth in hard turning operations. Mogaji et al. [10] determined the optimum parameters required for drilling brass using Response Surface Methodology (RSM) based on L9-A 34-2 fractional factorial design. Their results revealed that the process parameters have a high basic effect in influencing the response variable at %5 critical level beside tool on a zero assortment and that perfect method parameters can be cultivated at a widely appealing level during drilling.

Responses such as surface roughness, dimensional accuracy, cutting force, machining time, material removal rate (MMR), chip size, tool wear are typic emblematical parameters that may be used for a machining process optimization. For this reason, optimization tools have been applied to investigate the optimal process parameters and corresponding responses. Understanding the material behavior in low-lead brass alloys concerning chip fracture and formation mechanisms is vital in order to design candidate alloys for the substitution of conventional leaded brasses without compromising the reliability and performance of manufactured components [11]. Tripathy et al. [12] evaluated the effectiveness of optimizing multiple performance characteristics for PMEDM of H-11 die steel using copper electrode using Taguchi method in combination with Technique for order of preference by similarity to ideal solution and Grey Relational Analysis. They studied the effect of process variables such as powder concentration, peak current, pulse on time, duty cycle and gap voltage on response parameters such as material removal rate, tool wear rate, electrode wear ratio and surface roughness have been investigated using chromium powder mixed to the dielectric fluid.

Flat bottom drills are ideal for particular drilling operations or for flat bottom hole making without auxiliary finishing passes. These tools are favorable in thin plate, cross hole, irregular/rounded

surface, angled and half hole drilling operations. Figure 1 illustrates the various utilization of flat bottom drills.

In this study, an experimental investigation of the drilling operation on surface integrity characteristics of forged eco-friendly low-lead brass alloy using flat bottom drill cutting tool and application of techniques for order preference by similarity to ideal solution (TOPSIS) and Grey relational analysis methods in parametric optimization for solving multiple criteria (objective) process is carried out. Experimental data on dimensional accuracy, machining time, cutting forces, and the surface quality of the holes are analyzed to evaluate surface integrity of machined specimens. Analysis of variance (ANOVA) was performed to dispose the significance of the parameters at a 95% confidence interval. The forms of the obtained chips were studied in order to verify the optimization results.

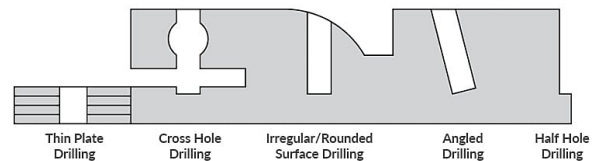


Figure 1. Schematic of the applications of bottom drill [13]

METHODOLOGY

EXPERIMENTAL PROCEDURE

In this study, the work material was CuZn38As (CW511L) low-lead brass alloy cylinders with 50 mm diameter and 200 mm length. The work materials were hot forged at $750 \pm 10^\circ \text{C}$ by 175-ton press with 9.1 m/s stroke velocity. Then forged specimens were considered for the machining experiments. Hence, first during rod extrusion and afterward during forging, the metal is worked twice under high stresses. The double working under tension compacts the metal and forms a dense and refined grain structure. Within that the tensile and shear strengths of the specimens are in this manner expanded. Despite wide range of the applications of these components, just a few studies have been focused on the machining of hot forged brass alloys. The chemical composition and mechanical properties of the test material is given in Table 1. The machining tests were carried out on Fanuc Robodrill α -D21MiB5. A two teeth carbide bottom drill with a diameter of 12 mm, axial rake angle of -5° , primary radial rake angle of 8° , secondary radial rake angle of 25° , 8° of relief angle and 40° of helix angle was used as a cutting tool as shown in Figure 2. During the investigation feed rate, $V_f=150, 300, 450, 600 \text{ mm/min}$, and cutting speed,

and $V_c=75, 115, 150, 190$ m/min was used with coolant flood. The dimensional accuracy of the machined parts has been evaluated by CMM from four points at a depth of 5 mm. The surface roughness of the drilled holes has been measured by Mitutoyo Surftest SJ-400 device and the average of five measurements are reported. The cutting forces have been measured using Kistler dynamometer type 9129AA at a sampling rate of 100 Hz for 10 seconds and the average thrust cutting forces during measurement have been reported in this study.

Table 1 Chemical composition of the studied brass alloy [14]

Composition	Cu	Zn	Pb	Fe	Ni	Al	As	Sn
CuZn38As (CW511L)	61.5	Rem	0.2	0.1	0.3	0.05	0.05	0.1
Technical specifications	Structure		Elasticity Modulus (GPa)		Density (g/cm ³)		Machinability	
	α, β		100		8.41		% 40	

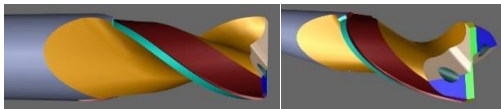


Figure 2. The utilized flat bottom drill

DETERMINATION OF OPTIMAL PROCESS PARAMETERS USING TOPSIS

Technique for order preference by similarity to ideal solution (TOPSIS) method is an optimization approach introduced by Hwang and Yoon. The basic concept of this method is the shortest and longest distance for the selected alternative (appropriate alternative) from the positive and negative ideal solution is a prerequisite for the answer, respectively. Positive ideal solution is a result that maximizes the benefit criteria and minimizes cost/unrewarding criteria. However, the negative ideal solution maximizes the benefit criteria and minimizes the cost/unrewarding criteria. A TOPSIS analysis is composed of below asserted steps:

Step 1: Development of a decision matrix having ‘ m ’ rows representing the alternatives and ‘ n ’ columns representing the attributes. The decision matrix can be expressed as in Equation (1) [15]:

$$DM = \begin{matrix} A_1 \\ A_2 \\ A_3 \\ \dots \\ A_m \end{matrix} \begin{bmatrix} a_{11} & a_{12} & a_{13} & \dots & a_{1n} \\ a_{21} & a_{22} & a_{23} & \dots & a_{2n} \\ a_{31} & a_{32} & a_{33} & \dots & a_{3n} \\ \dots & \dots & \dots & \dots & \dots \\ a_{m1} & a_{m2} & a_{m3} & \dots & a_{mn} \end{bmatrix} \quad (1)$$

where A_i ($i=1,2,\dots,m$) represents the possible alternatives; a_j ($j=1,2,\dots,n$) represents the attributes relating to alternative performance. In other words, a_{mn} is the performance of m^{th} alternative in relation to the n^{th} attribute.

Step 2: Calculation of the normalized matrix, which is demonstrated in Equation (2).

$$NM_{ij} = \frac{a_{ij}}{\sqrt{\sum_{i=1}^m a_{ij}^2}} \quad (2)$$

where NM_{ij} stands for the normalized performance of A_i with respect to attribute a_j .

Step 3: Calculation of the weighted normalized decision matrix $\phi=[\varphi_{ij}]$. The weight of each attribute was assumed to be w_j ($j=1,2,\dots,n$).

$$\phi = w_j \cdot NM_{ij} \quad (3)$$

$$\sum_{j=1}^n w_j = 1 \quad (4)$$

Step 4: Determination of the positive ideal (best) and negative ideal (worst) solutions by the following expressions:

$$\begin{aligned} A^+ &= \{(\max(\varphi_{ij})|j \in J), (\min(\varphi_{ij})|j \in J'|i \\ &= 1,2,\dots,m)\} \\ &= \{\varphi_1^+, \varphi_2^+, \dots, \varphi_n^+\} \end{aligned} \quad (5)$$

$$\begin{aligned} A^- &= \{(\min(\varphi_{ij})|j \in J), (\max(\varphi_{ij})|j \in J'|i \\ &= 1,2,\dots,m)\} \\ &= \{\varphi_1^-, \varphi_2^-, \dots, \varphi_n^-\} \end{aligned}$$

$$J, J' = \{j = 1,2,\dots,n|j\} \quad (6)$$

where J and J' are the associated with beneficial and unrewarding attributes.

Step 5: Determination of the distances for the solutions. The separation of each alternative from the ideal solution is given by n -dimensional Euclidean distance from the following Equation (8) and (9):

$$S_i^+ = \sqrt{\sum_{j=1}^n (\varphi_{ij} - \varphi_j^+)^2}; i = 1,2,\dots,m \quad (8)$$

$$S_i^- = \sqrt{\sum_{j=1}^n (\varphi_{ij} - \varphi_j^-)^2}; i = 1,2,\dots,m \quad (9)$$

Step 6: Calculation of the relative closeness to the ideal solution by Equation (10):

$$C_i^+ = \frac{S_i^-}{S_i^+ + S_i^-}; i = 1,2,\dots,m; 0 \leq C_i^+ \leq 1 \quad (10)$$

Step 7: Determination of the solution according to the ranking preference order including the most preferred and the least preferred solutions. The alternative with the largest relative closeness is the best choice.

DETERMINATION OF OPTIMAL PROCESS PARAMETERS USING GREY RELATION METHOD

This approach offers strategies for analysis and modelling of the system responses with constrained, incomplete information and characterized by means of random uncertainty. In this method, the whole considered performance objectives are incorporated into a single value that can be used as the single characteristic in optimization problems by data preprocessing.

Step 1: Grey relational generation

In this study, grey relational generating process, a linear normalization of the experimental results (S/N ratios), for responses were performed in the range of 0 and unity. y_{ij} is normalized as Z_{ij} ($0 \leq Z_{ij} \leq 1$) by the following formula. A linear data pre-processing method for the S/N ratio can be calculated by Equation (11):

$$Z_{ij} = \frac{y_{ij} - \min(y_{ij})}{\max(y_{ij}) - \min(y_{ij})}; i = 1, 2, \dots, n \quad (11)$$

Step 2: Calculation of the Grey relational coefficient. The relationship between the ideal (best) and actual normalized experimental results are calculated by Equation (12):

$$\gamma((k), y_i(k)) = \frac{\Delta \min + \xi \Delta \max}{\Delta o_j(k) + \xi \Delta \max} \quad (12)$$

where Z_{ij} is the sequence after the data processing, $j=1, 2, \dots, n$; n is the number of experimental data items and $k=1, 2, \dots, m$; m is the number of responses. ξ is the identification coefficient, defined in the range $0 \leq \xi \leq 1$. In this study, ξ is taken as equal to 0.5 in order to demonstrate equal parameter weighting.

Step 3: Calculation of difference values by the following Equation (13), (14) and (15).

$$\Delta o_j = ||y_0(k) - y_j(k)|| \quad (13)$$

$$\Delta \min = \min_i \min_k ||y_0(k) - y_j(k)|| \quad (14)$$

$$\Delta \max = \max_i \max_k ||y_0(k) - y_j(k)|| \quad (15)$$

where Δo_j is the absolute value of the difference between $y_0(k)$ and $y_j(k)$, $\Delta \min$ is the smallest value of $y_j(k)$, $\Delta \max$ is the largest value of $y_j(k)$, and $y_0(k)$ is the reference sequence ($y_0(k)=1, k=1, 2, \dots, m$); $y_j(k)$ is the specific comparison sequence.

Step 4: Calculation of the grey relation grade and ordering. The grey relational grade is determined by averaging the grey relational coefficient corresponding to each performance characteristic.

The overall performance characteristic of the multiple response process depends on the calculated grey relational grade. The grey relational grade can be expressed as,

$$\bar{\gamma}_j = \frac{1}{k} \sum_{i=1}^m \gamma_{ij} \quad (16)$$

where $\bar{\gamma}_j$ is the grey relational grade for the j^{th} experiment and k is the number of performance characteristics. This approach reduces a multiple response process optimization problem into a single response optimization situation with the objective function of an overall grey relational grade. The higher grey relational grade implies to the closer optimal corresponding result.

RESULTS AND DISCUSSIONS

The microstructure of the machined workpiece is demonstrated in Figure 3. The yellow and brown colors represent the α and β phases, with %72.14 and %27.86 of content, respectively. The presence of the β phase in the material microstructure simplifies the machining process.

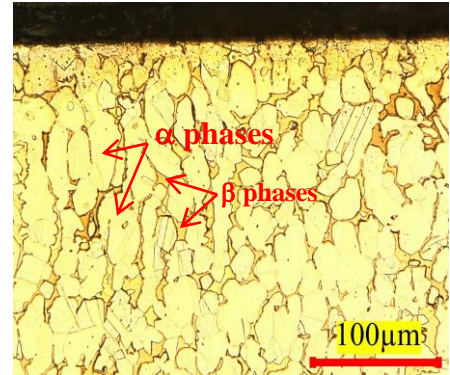


Figure 3. The microstructure of the machined workpiece

The maximum thrust force has been measured at 75 m/min and 600 mm/min of feed rate. However, the minimum value is measured at 190 m/min and 150 mm/min of cutting conditions. Increasing the cutting speed has led to the decrease in the cutting forces which can be attributed to the material softening at elevated temperatures. In contrary, increasing the feed rate has resulted in rising of the thrust force which is due to the increase of contact area during the cutting process. At higher cutting speeds with lower feed rates some vibrations and chatter marks besides to undesired cutting noises has been observed which can be attributed to the lower chip breakage capability and material removal evacuation. The amplitude of the vibrations of the related sound and chatter marks has been declined with the increase of feed rate. Figure 4 demonstrates

the measured cutting forces (thrust forces) in constant 150, 190 m/min of cutting speed and varying feed rate of 150, 300,450, 600 mm/min. Drilling responses related to different parameters has been taken as criteria attributes with 16 alternatives as demonstrated in Figure 5.

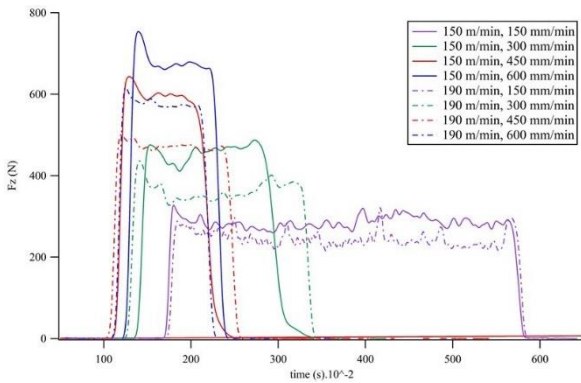
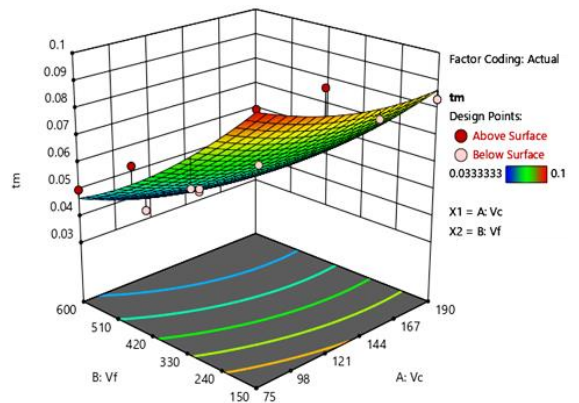
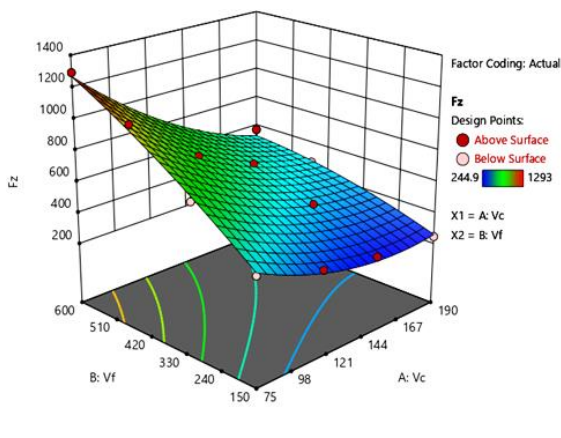
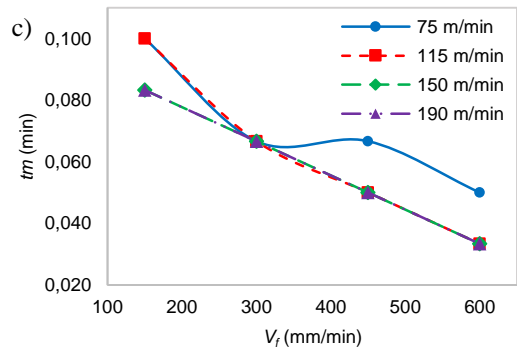
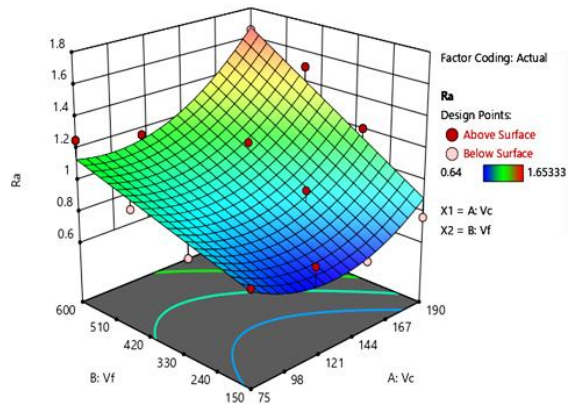
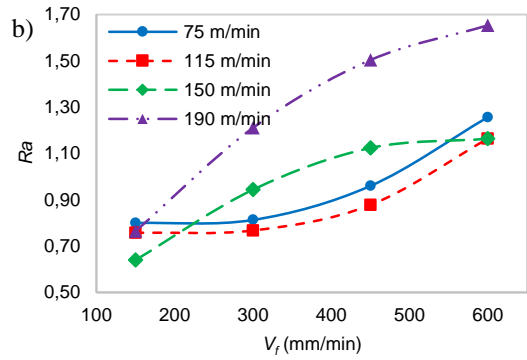
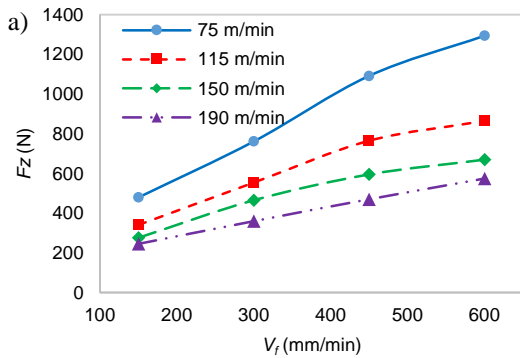


Figure 4. The measured cutting forces during drilling operation



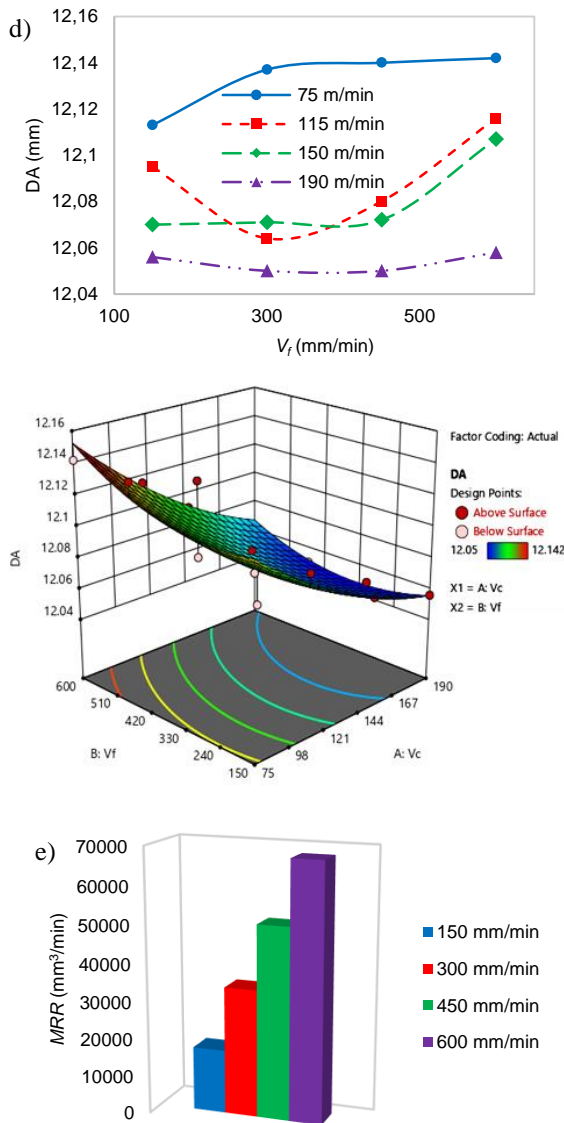


Figure 5. The measured cutting responses; a) thrust forces, b) surface roughness, c) machining time, d) hole diameter, e) material removal rate

As it seen from Figure 5a, maximum and minimum values of thrust force, 1293 N and 244.9 N, has been observed in 75 m/min, 190 m/min of cutting speed and 600 mm/min, 150 mm/min of feed rate, respectively. The thrust force has been boosted with the increase of feed rate and decrease in the cutting speed which can be attributed to the increase of the cutting contact area risen from them feed rate and softening of the metal in higher cutting speeds. Figure 5b demonstrates the measured average surface roughness of the holes. The maximum and minimum values of the surface roughness, 1.36 μm and 0.55 μm , has been observed in 150 mm/min, 75 m/min and 150 mm/min, 115 m/min, respectively. The feed marks have become evident and the surface roughness has been deteriorated with the increase of

feed rate. The increase of cutting speed from 75 m/min to 115 m/min has resulted in improvement of surface roughness which can be related to the softening of the metal and convenient cutting operation. In contrary, in 150 and 190 m/min of cutting speeds the surface roughness values have exhibited recrudescence which can be attributed to the chip breakage and chip removal of the cutting tool through flutes. Moreover, increasing the cutting speed has resulted into vibration and chatter marks. As it is seen from Figure 5c maximum and minimum values of machining time, 0.10 min and 0.033 min, has been observed in 75 m/min, 115 m/min of cutting speed and 600 mm/min, 600 mm/min of feed rate, respectively. Increasing the feed rate and cutting speed have led to the decrease in machining time which is verified with theoretical machining formulations. Figure 5d illustrates the dimensional deviation of the drilled holes. The maximum and minimum values have been measured as 12.145 and 12.05 mm, in 75 m/min, 600 mm/min, 190 m/min and 300 mm/min of cutting parameters, respectively. In general, increasing the feed rate has resulted in the increase of the dimensional accuracy error excluding 115 m/min of cutting speed and 150 mm/min of feed rate which can be attributed to the low chip breakage speed due to the low level of feed rate and leading to smearing of the chip to the hole surface. It is noteworthy to mention that the allowed tolerances of the desired hole dimensions are 12 ± 0.20 mm, and all the dimensions of the drilled holes are in the allowed tolerance range. Figure 5e shows the material removal rate of the experiments during drilling.

ANALYSIS OF VARIANCES

The statistical technique, analysis of variance (ANOVA), has been utilized in order to observe the influence of the experiment parameters on the machining results. Statistical significance of the fitted model and terms was evaluated by the P-values of ANOVA results. The analysis results are given in Tables 2 to 5 for machining time, diameter, surface roughness of the drilled hole and thrust force, respectively.

For the machining time, the predicted R^2 of 0.8946 is in reasonable agreement with the Adjusted R^2 of 0.9215. The Model F-value of 89.04 implies the model is significant. There is only a 0.01% chance that an F-value this large could occur due to noise. P-values less than 0.0500 indicate model terms are significant. In this case V_c , V_f are significant model terms. Values greater than 0.1000 indicate the model terms are not significant.

For the hole diameter, the predicted R^2 of 0.7665 is in reasonable agreement with the Adjusted R^2 of 0.8025. The Model F-value of 31.48 implies the

model is significant. There is only a 0.01% chance that an F-value this large could occur due to noise. P-values less than 0.0500 indicate model terms are significant. In this case V_c , V_f are significant model terms.

For the surface roughness of the drilled hole, the predicted R^2 of 0.5980 is in reasonable agreement with the Adjusted R^2 of 0.7154. The Model F-value of 19.85 implies the model is significant. There is only a 0.01% chance that an F-value this large could occur due to noise. P-values less than 0.0500 indicate model terms are significant. In this case V_c , V_f are significant model terms.

Last but not least, for the average thrust force, the predicted R^2 of 0.8212 is in reasonable agreement with the Adjusted R^2 of 0.8819; i.e. the difference is less than 0.2. The Model F-value of 56.99 implies the model is significant. There is only a 0.01% chance that an F-value this large could occur due to noise. P-values less than 0.0500 indicate model terms are significant. In this case V_c , V_f are significant model terms.

Table 2. ANOVA results of machining time (t_m)

Source	SS	df	MS	F-value	p-value
Model	0.0065	2	0.0032	89.04	< 0.0001
V_c	0.0003	1	0.0003	9.55	0.0086
V_f	0.0061	1	0.0061	168.53	< 0.0001
Residual	0.0005	13	0.0000		
Cor Total	0.0069	15			

Table 3. ANOVA results of dimensional accuracy error (DAE)

Source	SS	df	MS	F-value	p-value
Model	0.0134	2	0.0067	31.48	< 0.0001
V_c	0.0124	1	0.0124	58.12	< 0.0001
V_f	0.0010	1	0.0010	4.84	0.0464
Residual	0.0028	13	0.0002		
Cor Total	0.0162	15			

Table 4. ANOVA results of surface roughness (R_a)

Source	SS	df	MS	F-value	p-value
Model	0.9365	2	0.4683	19.85	0.0001
V_c	0.2221	1	0.2221	9.41	0.0090
V_f	0.7144	1	0.7144	30.28	0.0001
Residual	0.3067	13	0.0236		
Cor Total	1.24	15			

Table 5. ANOVA results of thrust force (F_z)

Source	SS	df	MS	F-value	p-value
Model	1.127E6	2	5.635E5	56.99	< 0.0001
V_c	5.200E5	1	5.200E5	52.59	< 0.0001
V_f	6.071E5	1	6.071E5	61.39	< 0.0001
Residual	1.285E5	13	9888.1		
Cor Total	1.256E6	15			

OPTIMIZATION USING TOPSIS AND GREY RELATION METHODS

The minimum of the machining time, dimensional accuracy error, surface roughness and plunging forces is desired considering the responses of drilling operation. Table 6 demonstrates the obtained experimental results and normalized machining responses. The weight of the machining time, dimensional accuracy error, surface roughness and cutting force have been taken as 0.3, 0.3, 0.25 and 0.15, respectively. The weight normalized and ideal solutions, their distance from optimum value and the ranks are given in Table 7.

The relative closeness to the optimum performance as for the ideal execution measure accomplishes the most extreme inclination preference and rank and is consequently considered as the best run. It is seen that run #4 is the best multiple performance characteristics having the highest preference order, hence it is the optimal setting followed by run #3 and #8.

Table 8 demonstrates the obtained experimental results and grey relation values. The weight of the machining time, dimensional accuracy error, surface roughness and cutting force have been taken equally as explained in section 2.3. The grey relational coefficients and relational grades and ranks are illustrated in Table 9. It is seen that run #4 is the best multiple performance characteristics having the highest rank is the optimal setting followed by run #3 and #2.

CHIP MORPHOLOGY

The experimental results of chip morphologies are shown in Figure 6. The chips of experiment 2, 3, 4, 5, 10, 11, 14, 15 and 16 are discrete. However, the chip forms of the rest experiments are curly. Considering the chips in terms of their form and breakability, the smallest discrete chips belong to run #4 which can remove the heat generated during machining are a robust verification to the obtained optimization results in both methods.

Table 6. Normalized TOPSIS

Run	Experimental results				Normalized results			
	t_m	DAE	Ra	F_z	t_m	DAE	Ra	F_z
1	0.100	0.113	0.80	478.7	0.379	0.299	0.188	0.178
2	0.067	0.137	0.81	760.9	0.253	0.363	0.191	0.282
3	0.067	0.14	0.96	1091	0.253	0.371	0.226	0.405
4	0.050	0.142	1.26	1293	0.190	0.376	0.296	0.480
5	0.100	0.095	0.76	340.8	0.379	0.252	0.178	0.126
6	0.067	0.064	0.77	554.3	0.253	0.170	0.181	0.206
7	0.050	0.08	0.88	764.9	0.190	0.212	0.206	0.284
8	0.033	0.116	1.16	864.7	0.126	0.307	0.274	0.321
9	0.083	0.07	0.64	275.6	0.316	0.186	0.151	0.102
10	0.067	0.071	0.94	465	0.253	0.188	0.222	0.173
11	0.050	0.072	1.12	595.2	0.190	0.191	0.264	0.221
12	0.033	0.107	1.16	669.8	0.126	0.284	0.274	0.249
13	0.083	0.056	0.76	244.9	0.316	0.148	0.180	0.091
14	0.067	0.05	1.21	359.5	0.253	0.133	0.285	0.133
15	0.050	0.05	1.50	470.3	0.190	0.133	0.354	0.175
16	0.033	0.058	1.65	574.9	0.126	0.154	0.389	0.213

Table 7. Weight normalized and ideal solutions (Best/ Worst) distance

Run	Weight Normalized TOPSIS				Ideal Solution Distance			Rank
	t_m	DAE	Ra	F_z	Si+	Si-	Ci+	
1	0.114	0.090	0.047	0.044	0.121	0.099	0.451	10
2	0.076	0.109	0.048	0.071	0.080	0.108	0.575	13
3	0.076	0.111	0.057	0.101	0.059	0.111	0.654	15
4	0.057	0.113	0.074	0.120	0.030	0.125	0.806	16
5	0.114	0.076	0.045	0.032	0.133	0.103	0.436	8
6	0.076	0.051	0.045	0.051	0.113	0.083	0.425	6
7	0.057	0.064	0.052	0.071	0.085	0.079	0.482	11
8	0.038	0.092	0.068	0.080	0.053	0.098	0.648	14
9	0.095	0.056	0.038	0.026	0.138	0.107	0.437	9
10	0.076	0.056	0.056	0.043	0.111	0.082	0.424	5
11	0.057	0.057	0.066	0.055	0.093	0.071	0.434	7
12	0.038	0.085	0.068	0.062	0.070	0.089	0.558	12
13	0.095	0.045	0.045	0.023	0.142	0.103	0.422	4
14	0.076	0.040	0.071	0.033	0.122	0.076	0.384	3
15	0.057	0.040	0.088	0.044	0.108	0.060	0.359	1
16	0.038	0.046	0.097	0.053	0.094	0.054	0.363	2

Table 8. Grey relational generation values

Run	Experimental results				Grey relational generation values			
	t_m	DAE	Ra	F_z	t_m	DAE	Ra	F_z
1	0.100	0.113	0.80	478.7	0.000	0.315	0.842	0.777
2	0.067	0.137	0.81	760.9	0.500	0.054	0.829	0.508
3	0.067	0.14	0.96	1091	0.500	0.022	0.684	0.193
4	0.050	0.142	1.26	1293	0.750	0.000	0.391	0.000
5	0.100	0.095	0.76	340.8	0.000	0.511	0.885	0.909
6	0.067	0.064	0.77	554.3	0.500	0.848	0.875	0.705
7	0.050	0.08	0.88	764.9	0.750	0.674	0.766	0.504
8	0.033	0.116	1.16	864.7	1.000	0.283	0.484	0.409
9	0.083	0.07	0.64	275.6	0.250	0.783	1.000	0.971
10	0.067	0.071	0.94	465	0.500	0.772	0.701	0.790
11	0.050	0.072	1.12	595.2	0.750	0.761	0.523	0.666
12	0.033	0.107	1.16	669.8	1.000	0.380	0.484	0.595
13	0.083	0.056	0.76	244.9	0.250	0.935	0.878	1.000
14	0.067	0.05	1.21	359.5	0.500	1.000	0.438	0.891
15	0.050	0.05	1.50	470.3	0.750	1.000	0.148	0.785
16	0.033	0.058	1.65	574.9	1.000	0.913	0.000	0.685

Table 9. Grey relational coefficient and grey relational grade values

Run	Doi				Grey Relation Coefficient				GRG	Rank
	t_m	DAE	Ra	F_z	t_m	DAE	Ra	F_z		
1	1.000	0.685	0.158	0.223	0.333	0.422	0.760	0.691	0.552	13
2	0.500	0.946	0.171	0.492	0.500	0.346	0.745	0.504	0.524	14
3	0.500	0.978	0.316	0.807	0.500	0.338	0.613	0.382	0.458	15
4	0.250	1.000	0.609	1.000	0.667	0.333	0.451	0.333	0.446	16
5	1.000	0.489	0.115	0.091	0.333	0.505	0.813	0.845	0.624	8
6	0.500	0.152	0.125	0.295	0.500	0.767	0.800	0.629	0.674	6
7	0.250	0.326	0.234	0.496	0.667	0.605	0.682	0.502	0.614	10
8	0.000	0.717	0.516	0.591	1.000	0.411	0.492	0.458	0.590	12
9	0.750	0.217	0.000	0.029	0.400	0.697	1.000	0.945	0.760	2
10	0.500	0.228	0.299	0.210	0.500	0.687	0.626	0.704	0.629	7
11	0.250	0.239	0.477	0.334	0.667	0.676	0.512	0.599	0.614	11
12	0.000	0.620	0.516	0.405	1.000	0.447	0.492	0.552	0.623	9
13	0.750	0.065	0.122	0.000	0.400	0.885	0.804	1.000	0.772	1
14	0.500	0.000	0.563	0.109	0.500	1.000	0.471	0.821	0.698	4
15	0.250	0.000	0.852	0.215	0.667	1.000	0.370	0.699	0.684	5
16	0.000	0.087	1.000	0.315	1.000	0.852	0.333	0.614	0.700	3

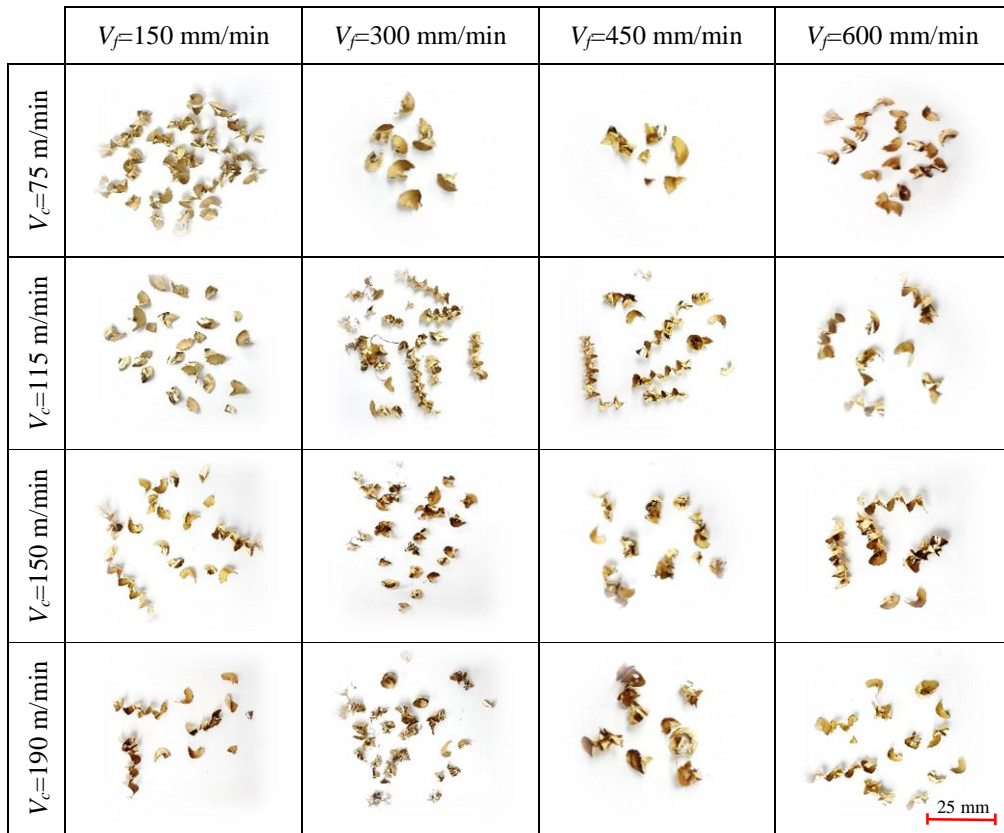


Figure 6. The chip morphology of the drilling experiments

CONCLUSION

In this paper, an experimental data has been produced and used in order to evaluate the machining performance and optimize the cutting conditions in drilling of forged ecofriendly low-lead brass alloy

with a special form bottom drill cutting tool. Through the results obtained above, the following conclusions are illustrated in below:

The ANOVA analysis revealed that the feed rate is the most significant factor affecting machining

time, surface roughness and cutting force. However, cutting speed played the major role in drilled hole dimensional accuracy.

The machining performance have been evaluated using TOPSIS and Grey relation analysis. Optimization of the drilling operation has yielded to minimum production time, cutting force, dimensional error, and surface roughness.

Both TOPSIS and Grey relational approaches have been used for optimization, they concluded with the same solution for drilling operation. The analysis in this paper reveals that TOPSIS and Grey relational concepts can be efficiently integrated towards a flexible compatible multi-response optimization methodology. The macro analysis of the obtained chips verified the optimization results considering due to the formation of small chip sizes during machining.

Acknowledgements

The authors thank TUBITAK (The Scientific and Technological Research Council of Turkey) for partially supporting this work under project number 118C069.

ÖZET

Bu araştırma, düz matkap takımı kullanılarak dövülmüş çevre dostu az kurşunlu pirinç alaşımının yüzey bütünlüğü özellikleri üzerindeki delme işleminin deneysel incelemesini ve ideal çözüme (TOPSIS) benzerlik ile sıra tercihi ve Grey orantı analiz tekniklerinin uygulanmasını ile çoklu çözüm için parametrik optimizasyon sunmaktadır. Boyutsal doğruluk, işleme süresi, kesme kuvvetleri ve deliklerin yüzey kalitesi hakkındaki deneysel veriler, işlenmiş numunelerin yüzey bütünlüğünü değerlendirmek için analiz edilmiştir. Parametrelerin önemini % 95 güven aralığında elden çıkarmak için varyans analizi (ANOVA) gerçekleştirilmiştir. Her iki optimizasyon aracı da aynı kesme parametreleriyle sonuçlanmıştır. Elde edilen talaş formlarının analizi optimizasyon sonuçlarını doğrulamıştır.

Anahtar Kelimeler: TOPSIS, Grey ilişki analizi, optimizasyon.

REFERENCES

1. Engineering Designer 30(3): 6–9, May–July 2004
2. N. Zoghipour, E. Tascioglu, G. Atay, Y. Kaynak, Machining-induced surface integrity of holes drilled in lead-free brass alloy, *Procedia CIRP*, 87; 2020, p. 148-152.
3. Stagnation Time, Composition, pH, and Orthophosphate Effects on Metal Leaching from Brass. Washington DC: United States Environmental Protection Agency, 1996, p. 7. EPA/600/R-96/103.
4. F. Schultheiss, D. Johansson, V. Bushlya, J. Zhou, K. Nilsson, J. Ståhla, Comparative Study on the Machinability of Lead-Free Brass, *Journal of Cleaner Production*, 149; 2017, p. 366-377
5. A. A. Rahman, A. Mamat, A. Wagiman, Effect of Machining Parameters on Hole Quality of Micro Drilling for Brass, *Modern applied sciences*, 3(5), 2009.
6. M. Timata, C. Saikaew. Influences of spindle speed and feed rate on exit burr height and workpiece diameter in drilling forging brass, *Solid state phenomena*, 279; 2018, p. 67-71.
7. H. Kato, S. Nakata, N. Ikenaga, H. Improvement of chip evacuation in drilling of lead-free brass using micro drill, *International journal of automation technology*, 8; 2014.
8. H. A. Youssef, M. Y. Al-Makky, R. A. Al-Kadeem, I. S. Shyha, Burr formation in drilling of miniature holes in brass, 8th International Conference on Production Engineering Design and Control, PEDAC, 2004.
9. J. Hua, R. Shivpuri, X. Cheng, V. Bedekar, Y. Matsumoto, F. Hashimoto, T. R. Watkins. Effect of feed rate, workpiece hardness and cutting edge on subsurface residual stress in the hard turning of bearing steel using chamfer + hone cutting edge geometry, *Materials Science and Engineering A*, 394; 2005, p. 238–248.
10. P. B. Mogaji, I. A. Famurewa. Investigating optimum parameters required for drilling brass using response surface methodology, *Journal of emerging trends in engineering and applied sciences*, 8(1); 2017, p. 37 – 42.
11. Toulfatzis, A.; Pantazopoulos, G.; Paipetis, A. Fracture behavior and characterization of lead-free brass alloys for machining applications. *J. Mater. Eng. Perform*, 23; 2014, p. 3193–3206.
12. S. Tripathy a, D.K. Tripathy, Multi-attribute optimization of machining process parameters in powder mixed electro - discharge machining using TOPSIS and grey relational analysis, *Engineering Science and Technology, an International Journal*, 19 ; 2016, p. 62–70.
13. <https://www.harveyperformance.com/>
14. <https://www.sarbak.com.tr/>
15. V. S. Gadakh, Parametric optimization of wire electrical discharge machining using topsis method, *Advances in Production Engineering & Management* 7(3); 2012, p. 157-164.